Inorg. Chem. **2006**, *45*, 821–827

Structure and Properties of Dinuclear [Ru^{II}([*n*]aneS_4)] Complexes of 3,6-Bis(2-pyridyl)-1,2,4,5-tetrazine

Mike Newell, James D. Ingram, Timothy L. Easun, Steven J. Vickers, Harry Adams, Michael D. Ward, and Jim A. Thomas*

Department of Chemistry, University of Sheffield, Sheffield, S3 7HF, U.K.

Received July 11, 2005

The synthesis of dinuclear [Ru^{II}([*n*]aneS_4)] (where $n = 12$, 14) complexes of the bridging ligand 3,6-bis(2-pyridyl)-1,2,4,5-tetrazine are reported. The X-ray structures of both of the new complexes are compared to a newly obtained structure for a dinuclear [Ru^{II}([9]aneS_3)]-based analogue, whose synthesis has previously been reported. A comparison of the electrochemistry of the three complexes reveals that the first oxidation of the [Ru^{II}([*n*]aneS_4)]-based systems is a ligand-based couple, indicating that the formation of the radical anion form of the bridging ligand is stabilized by metal center coordination. Spectroelectrochemistry studies on the mixed-valence form of the new complexes suggest that they are Robin and Day Class II systems. The electrochemical and electronic properties of these complexes is rationalized by a consideration of the π-bonding properties of thiacrown ligands.

Introduction

For nearly 40 years, the electronic properties of ligand-bridged dinuclear mixed valence (MV) transition metal complexes, particularly those of $d^{5/6}$ metal centers, have attracted a huge amount of attention.[1] The Creutz−Taube (CT) ion is probably the most studied of such systems.[2] For over two decades, the extent of electronic delocalization within the CT ion was an issue of great debate, with conflicting evidence suggesting that the system was either Robin and Day[3] Class II (valence localized electron hopping) or Class III (valence delocalized).[1a,1d,4] Following Stark spectroscopy[5] studies, it was concluded that the complex was Class III,[6] and further evidence in support of this conclusion was provided by later detailed DFT calculations;[7] however, more recently it has been suggested that its properties are more appropriately described by a new classification, Class II/III.[8]

The CT ion has been the template for a huge variety of oligonuclear complexes. The electrochemical and photophysical properties of these complexes have been thoroughly investigated, and their fascinating electron transfer, ET, properties mean that they have functioned as prototypes for a multiplicity of molecular devices.[9] However, although it is known that altering coordinated donor ligands can have significant effects on the properties of such systems,[10] virtually all this work has exclusively involved nitrogen-donor ligands.

Given that many biological ET systems are based on transition metals coordinated to sulfur donor sites,[11] we have been investigating how the inclusion of sulfur-donating thiacrown ligands modulate the ET properties of MV com-

* To whom correspondence should be addressed. E-mail: james.thomas@sheffield.ac.uk.

(1) (a) Creutz, C. *Prog. Inorg. Chem.* **1983**, *30*, 1. (b) Meyer, T. J. *Acc. Chem. Res* **1989**, *22*, 163. (c) *Electron Transfer in Inorganic, Organic and Biological Systems*; Bolton, J. R., Mataga, N., McLendon, G., Eds.; Advances in Chemistry Series 228, American Chemical Society: Washington, DC, 1991. (d) Crutchley, R. J. *Adv. Inorg. Chem.* **1994**, *41*, 273. (e) Brunschwig; B. S.; Sutin, N. *Coord. Chem. Rev.* **1999**, *187*, 233. (f) Kaim, W.; Klein, A.; Glöckle, M. *Acc. Chem. Res.* **2000**, *33*, 755.

(2) (a) Creutz, C.; Taube, H. *J. Am. Chem. Soc.* **1969**, *91*, 3988. (b) Creutz, C.; Taube, H. *J. Am. Chem. Soc.* **1973**, *95*, 1086. (c) Taube, H. *Angew. Chem., Int. Ed. Engl.* **1984**, *23*, *329.*

(3) Robin, M. B. Day P. *Adv. Inorg. Chem. Radiochem.* **1967**, *10*, 247.

(4) Citrin, P. *J. Am. Chem. Soc.* **1973**, *95*, 6472. Strekas, T. C.; Spiro, T. G. *Inorg. Chem.* **1976**, *15*, 974. Beattie, J. K.; Hush, N. S.; Taylor, P. R.; Ralston, C. L.; White, A. H. *J. Chem. Soc., Dalton Trans.* **1977**, 1121. Furholtz, U.; Burgi, H.-B.; Wagner, F. E.; Stebler, A.; Ammeter, J. H.; Krausz, E.; Clark, R. J. H.; Stead, M. J.; Ludi, A. *J. Am. Chem. Soc.* **1984**, *106*, 121. Stebler, A.; Ammeter, J. H.; Furholtz, U.; Ludi, A. *Inorg. Chem.* **1984**, *23*, 2764. Best, S. P.; Clark, R. J. H.; McQueen, R. C. S.; Joss, S. *J. Am. Chem. Soc.* **1989**, *111*, 548.

(5) Bublitz, G. U.; Boxer, S. G. *Annu. Rev. Phys. Chem.* **1997**, *48*, 213.

(6) Oh, D.; Sano, M.; Boxer, S. G. *J. Am. Chem. Soc.* **1991**, *113*, 6880.

(7) Bencini, A.; Ciofini, I.; Daul, C. A.; Feretti, A. *J. Am. Chem. Soc.* **1999**, *121*, 11418.

(8) Demadis, K. D.; Hartshorn, C. M.; Meyer, T. J. *Chem. Rev.* **2001**, *101*, 2655. Brunschwig, B. S.; Creutz, C.; Sutin, N. *Chem. Soc. Rev.* **2002**, *31*, 168.

(9) Ward, M. D. *Chem. Soc. Rev.* **1995**, *24*, 121. Balzani, V.; Juris, A.; Venturi, M.: Campagna, S.; Serroni, S. *Chem. Rev.* **1996**, *96*, 759. Launay, J. P. *Chem. Soc. Rev.* **2001**, *30*, 386. Ward, M. D.; Barigelletti, F. *Coord. Chem. Rev.* **2001**, *216*−*217*, 127.

10.1021/ic051151b CCC: $33.50
Published on Web 12/24/2005

Scheme 1

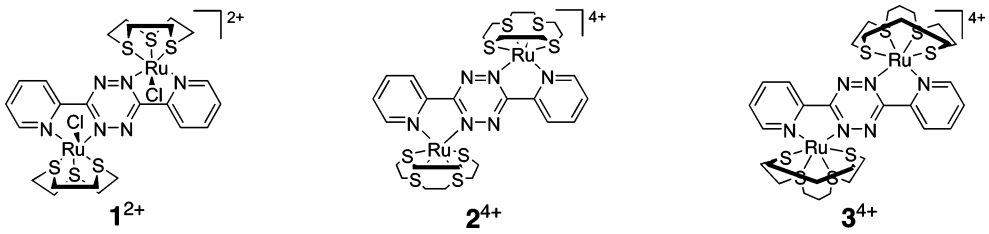

Table 1. Summary of Crystallographic Data for [**1**]$(PF_6)_2$, [**2**]$(PF_6)_4$, and [**3**]$(PF_6)_4$

	[**1**]$(PF_6)_2$	[**2**]$(PF_6)_4$·$4CH_3NO_2$	[**3**]$(PF_6)_4$·$4CH_3NO_2$
empirical formula	$C_{24}H_{32}Cl_2F_{12}N_6P_2Ru_2S_6$	$C_{32}H_{52}F_{24}N_{10}O_8P_4Ru_2S_8$	$C_{36}H_{60}F_{24}N_{10}O_8P_4Ru_2S_8$
M_r	1159.9	1743.34	1799.44
cryst syst	triclinic	monoclinic	triclinic
space group	$P\bar{1}$	$P2/c$	$P\bar{1}$
cryst dimensions/mm	0.38 × 0.23 × 0.12	0.43 × 0.22 × 0.12	0.28 × 0.07 × 0.07
a/Å	10.2695(10)	16.6771(12)	11.398(5)
b/Å	10.4904(10)	10.9629(8)	12.470(6)
c/Å	14.0838(14)	19.3193(14)	16.302(7)
α/°	110.382(2)	90	68.837(8)
β/°	100.025(2)	113.4250(10)	72.709(9)
γ/°	93.354(2)	90	71.477(8)
U/Å^3	1388.8(2)	3241.0(4)	2004.8(15)
Z	1	2	1
Dc/Mg/m^3	1.387	1.786	1.490
F(000)	574	1740	902
μ(Mo Kα)/mm^{-1}	0.985	0.942	0.764
final R1 [$I > 2\sigma(I)$] (all data)	0.0806 (0.0961)	0.0670 (0.0833)	0.0915 (0.1226)
final wR2 [$I > 2\sigma(I)$] (all data)	0.2274(0.2493)	0.1929 (0.2051)	0.2252 (0.2404)

plexes. Our initial studies, involving the facially coordinating tridentate ligand [9]aneS_3, resulted in the isolation of oligonuclear complexes, such as **1** (Scheme 1), displaying intense electronic coupling.[12,13] Recently, we have developed routes to the synthesis of mononuclear complexes incorporating [([n]aneS_4)Ru] metal centers.[14] Herein, we outline the syntheses and properties of analogous dinuclear complexes, bridged by the ligand 3,6-bis(2-pyridyl)-1,2,4,5-tetrazine, bpta.[15]

Results and Discussion

Synthetic and Structural. Although the synthesis of [(RuCl[9]aneS_3)$_2$bpta]$(PF_6)_2$, [**1**]$(PF_6)_2$, has been reported before,[12] we have developed a more convenient synthesis that does not require column chromatography. The synthesis of the new dinuclear thiacrown complexes [(Ru[12]aneS_4)$_2$-bpta]$(PF_6)_4$, [**2**]$(PF_6)_4$, and [(Ru[14]aneS_4)$_2$bpta]$(PF_6)_4$, [**3**]-$(PF_6)_4$, Scheme 1, were carried out through the reaction of bpta with the appropriate [(Ru[n]aneS_4)Cl(DMSO)]$^+$ starting material.[14] In all three cases, it was found that addition of NH_4PF_6 to a hot solution of the reaction mixture led to the precipitation of analytically pure products that required no further workup. The solid-state structures of all three products were confirmed by X-ray crystallography, Table 1.

The structure of the cation $\mathbf{1}^{2+}$ is shown in Figure 1, and selected bond lengths and angles are summarized in Table 2.

The two ruthenium(II) ions of $\mathbf{1}^{2+}$ take up distorted octahedral coordination geometry and lie in one plane with

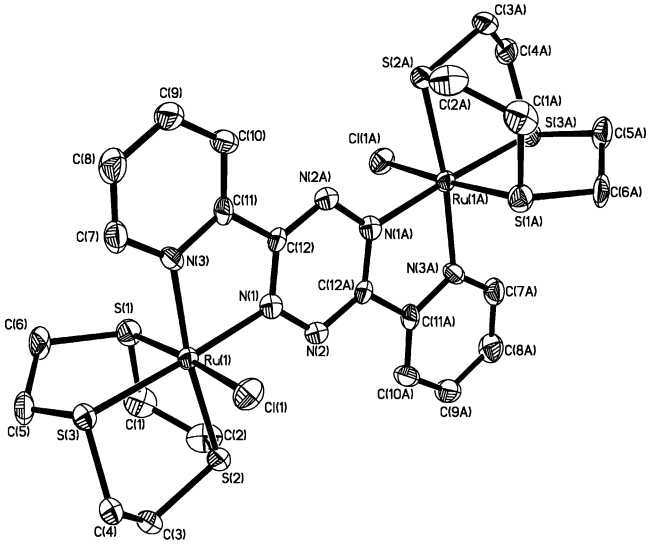

Figure 1. Diagram of structure of the cation of [**1**]$(PF_6)_2$ showing thermal ellipsoids. Hydrogen atoms, solvent, and counterions omitted for clarity.

(10) de la Rosa, R.; Chang, P. J.; Salaymeh, F.; Curtis, J. C. *Inorg. Chem.* **1985**, *24*, 4229. Salaymeh, F.; Berhane, S.; Yusof, R.; de la Rosa, R.; Fung, E. Y.; Matamoros, R.; Lau, K. W.; Zheng, Q.; Kober, E. M.; Curtis, J. C. *Inorg. Chem.* **1993**, *32*, 3895.
(11) Soloman, E. I.; Brunold, T. C.; Davies, M. I.; Kemsley, J. N.; Lee, S.-K.; Lehnert, N.; Neese, F.; Skulan, A. J.; Yang, Y.-S.; Zhou, J. *Chem. Rev.* **2000**, *100*, 235.
(12) Roche, S.; Yellowlees, L. J.; Thomas, J. A. *Chem. Commun.* **1998**, 1429. Araújo, C. S.; Drew, M. G. B.; Félix, V.; Jack, L.; Madureira, J.; Newell, M.; Roche, S.; Santos, T. M.; Thomas, J. A.; Yellowlees, L. *Inorg. Chem.* **2002**, *41*, 2250.
(13) Shan, N.; Vickers, S.; Adams, H.; Ward, M. D.; Thomas, J. A. *Angew. Chem., Int. Ed.* **2004**, *43*, 3938.
(14) Adams, H.; Amado, A. M.; Félix, V.; Mann, B. E.; Antelo-Martinez, J.; Newell, M.; Ribeiro-Claro, P. J. A.; Spey S. E.; Thomas, J. A. *Chem. Eur. J.* **2005**, *11*, 2031.
(15) Libman, D. D.; Slack, R. *J. Chem. Soc.* **1956**, 2253. Geldard, J. F.; Lions, F. *J. Org. Chem.* **1965**, *30*, 318.

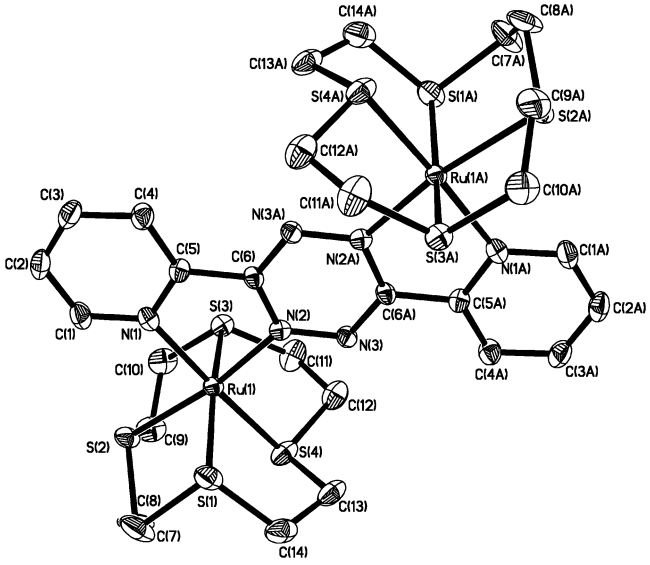

Figure 2. Diagram of structure of the cation of [**2**]$(PF_6)_4$ showing thermal ellipsoids. Hydrogen atoms, solvent, and counterions omitted for clarity.

Table 2. Selected Bond Lengths and Angles for Complex [**1**]$(PF_6)_2$

Distances and Bond Lengths (Å)	
Ru(1)···Ru(2)	6.702
Ru(1)−N(1)	2.011(5)
Ru(1)−N(3)	2.098(5)
Ru(1)−S(1)	2.3033(17)
Ru(1)−S(2)	2.3111(16)
Ru(1)−S(3)	2.3389(16)
Ru(1)−Cl(1)	2.4177(17)
Angles (deg)	
N(1)−Ru(1)−S(1)	92.81(15)
N(1)−Ru(1)−S(2)	95.15(15)
N(1)−Ru(1)−S(3)	176.56(15)
N(3)−Ru(1)−S(1)	94.89(15)
N(3)−Ru(1)−S(2)	172.87(14)
N(3)−Ru(1)−S(3)	98.28(14)
N(1)−Ru(1)−N(3)	78.30(2)
S(1)−Ru(1)−Cl(1)	175.20(6)
S(2)−Ru(1)−Cl(1)	91.74(6)
S(3)−Ru(1)−Cl(1)	87.28(6)
S(1)−Ru(1)−S(2)	88.22(6)
S(1)−Ru(1)−S(3)	87.92(6)
S(2)−Ru(1)−S(3)	88.23(6)
N(1)−Ru(1)−Cl(1)	91.98(15)
N(3)−Ru(1)−Cl(1)	85.70(15)

the bpta ligand. Thanks largely to the conflicting coordination demands of the thiacrown and the bidentate nitrogen sites of the bpta ligand, the three trans angles at the ruthenium(II) site show a slight variation away from ideal octahedral geometry: the two trans angles of N−Ru−S are 176.56(15)° and 172.87(14)°, while the S−Ru−Cl angle is 175.20(6)°. As might be expected, the five-membered chelate ring that results from the bidentate coordination of the N-donor atoms of the bpta ligand results in a bite angle of 78.30(2)°, which is more acute than the idealized 90°. There are slight differences between the Ru−S bonds with Ru(1)−S(1) being the shortest—2.3033(17) Å—probably due to the greater trans effect of chlorine.

The structure of the cation $\mathbf{2}^{4+}$, showing thermal ellipsoids, is displayed in Figure 1, and selected bond lengths and angles are summarized in Table 3.

As for $\mathbf{1}^{2+}$, both ruthenium(II) ions are in a distorted octahedral geometry and lie in one plane with the bpta ligand.

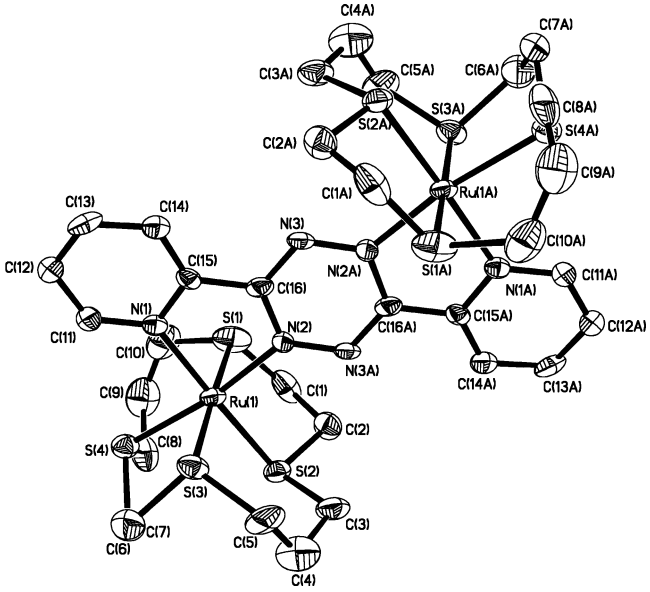

Figure 3. Diagram of structure of the cation of [**3**]$(PF_6)_4$ showing thermal ellipsoids. Hydrogen atoms, solvent, and counterions omitted for clarity.

However, there are now significant differences in the three trans angles at the ruthenium(II) site with all three showing significant deviation from 180°. These distortions are due to a previously observed phenomenon; the steric demands of coordinating all four donor S atoms of a macrocycle possessing a relatively small host cavity.[14,16]

The metal−sulfur bond lengths show slight differences, e.g., Ru(1)−S(3) = 2.3764(14) Å compared to Ru(1)−S(4) = 2.3140(15) Å, this too is largely assigned to distortions due to the relatively small size of the [12]-ane-S_4 coordination cavity.

While the structure of [**3**]$(PF_6)_4$ is very similar to that of [**2**]$(PF_6)_4$, there is clear evidence that coordination of the larger [14]-ane-S_4 ligand produces less distortion away from idealized octahedral geometry (Figure 3, Table 4). For example, although the angle in the five-membered chelate ring that arises from the bidentate coordination of the two N-donors of the bpta ligand is still small (79.2(3)°), the three trans angles in **3** show a range of ca. 6.25° compared to the analogous figure for **2** of over 12.5°.

Furthermore, compared to **2**, the metal−sulfur bond lengths in **3** now show very small differences, e.g., Ru(1)−S(3) = 2.338(2) Å compared to Ru(1)−S(2) = 2.303(2) Å. These slight differences are probably due to trans effects, as S(1) is trans to S(3) while N(1) is trans to S(2). Clearly, as has been observed before,[14,17] [14]aneS_4 coordination produces less distortion away from idealized octahedral geometries compared to the smaller-diameter [12]aneS_4.

In previous studies on mononuclear complexes of thiacrown macrocycles,[14] we have found that lone-pair inversion of sulfur donors can lead to three possible invertomer conformations, which we labeled ***a***, ***b***, and ***c***—Scheme 2.

(16) (a) Goodfellow, B. J.; Pacheco, S. M. D.; Pedrosa de Jesus, J.; Felix, V.; Drew, M. G. B. *Polyhedron* **1997**, *16*, 3293. (b) Santos, T. M.; Goodfellow, B. J.; Madureira, J.; Pedrosa de Jesus, J.; Felix, V.; Drew, M. G. B. *New J. Chem.* **1999**, *23*, 1015.

(17) Blake, A. J.; Reid, G.; Schröder, M. *J. Chem. Soc., Dalton. Trans* **1989**, 1675.

Table 3. Selected Distances, Bond Lengths, and Angles for Complex [**2**](PF$_6$)$_4$

Distances and Bond Length (Å)	
Ru(1)···Ru(2)	6.806
Ru(1)−S(1)	2.3704(15)
Ru(1)−S(2)	2.3276(13)
Ru(1)−S(3)	2.3764(14)
Ru(1)−S(4)	2.3140(15)
Ru(1)−N(1)	2.113(5)
Ru(1)−N(2)	2.038(4)
Angles (deg)	
N(1)−Ru(1)−N(2)	79.2(3)
N(1)−Ru(1)−S(1)	94.97(18)
N(1)−Ru(1)−S(2)	177.96(18)
N(1)−Ru(1)−S(3)	88.28(18)
N(1)−Ru(1)−S(4)	92.59(19)
N(2)−Ru(1)−S(1)	87.19(19)
N(2)−Ru(1)−S(2)	98.7(2)
N(2)−Ru(1)−S(3)	95.06(19)
N(2)−Ru(1)−S(4)	171.71(19)
S(1)−Ru(1)−S(2)	85.05(9)
S(1)−Ru(1)−S(3)	176.34(8)
S(1)−Ru(1)−S(4)	92.14(9)
S(2)−Ru(1)−S(3)	91.76(8)
S(2)−Ru(1)−S(4)	89.45(8)
S(3)−Ru(1)−S(4)	86.04(8)

Table 4. Selected Distances, Bond Lengths, and Angles for Complex [**3**](PF$_6$)$_4$

Distances and Bond Length (Å)	
Ru(1)···Ru(2)	6.708
Ru(1)−S(1)	2.331(2)
Ru(1)−S(2)	2.303(2)
Ru(1)−S(3)	2.338(2)
Ru(1)−S(4)	2.326(2)
Ru(1)−N(1)	2.080(6)
Ru(1)−N(2)	2.017(6)
Angles (deg)	
N(1)−Ru(1)−N(2)	78.18(17)
N(1)−Ru(1)−S(1)	97.24(13)
N(1)−Ru(1)−S(2)	91.96(12)
N(1)−Ru(1)−S(3)	95.98(12)
N(1)−Ru(1)−S(4)	177.40(12)
N(2)−Ru(1)−S(1)	94.73(12)
N(2)−Ru(1)−S(2)	170.13(13)
N(2)−Ru(1)−S(3)	95.06(12)
N(2)−Ru(1)−S(4)	99.38(12)
S(1)−Ru(1)−S(2)	86.14(5)
S(1)−Ru(1)−S(3)	164.91(15)
S(1)−Ru(1)−S(4)	83.78(6)
S(2)−Ru(1)−S(3)	86.18(5)
S(2)−Ru(1)−S(4)	90.49(5)
S(3)−Ru(1)−S(4)	83.32(5)

Scheme 2. Three Possible Conformations of S-Donors in Coordinated [*n*]aneS$_4$ Ligands

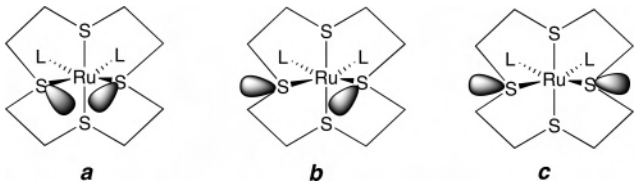

The two new dinuclear complexes take up conformation ***b***. In analogous mononuclear complexes, this was found to be the lowest-energy conformation for coordinated [14]aneS$_4$, while for the [12]aneS$_4$ conformation, ***b*** was found to be only slightly higher in energy than conformation ***c***. At room temperature, the ^{1}H NMR spectrum of **2**$^{4+}$ is consistent with the assigned structure of the complexes, while that of **3**$^{4+}$ shows some evidence of exchange broadening. Again, this observation is consistent with previous studies on analogous mononuclear complexes[14,18] and indicative of invertomer interconversion.

Table 5. UV/Visible Absorption Data for **1**−**3**

complex[a]	λ_{max} (nm)	ϵ (**dm**^{3} mol^{-1} cm^{-1})	assignment
1^{2+} [b]	302	34 900	$\pi-\pi^*$
	751	22 800	MLCT
2^{4+}	308	37 500	$\pi-\pi^*$
	528	12 000	MLCT
	716	22 000	MLCT
3^{4+}	327	35 200	$\pi-\pi^*$
	628	21 100	MLCT
	710	sh	MLCT

[a] Hexafluorophosphate salts in acetonitrile. [b] Figures from ref 12.

UV/vis Spectroscopic Studies. The UV/vis spectra of the hexafluorophosphate salts of **2**$^{4+}$ and **3**$^{4+}$ were recorded in acetonitrile solvent, and details are summarized in Table 5. To aid comparisons, data for **1**$^{2+}$ are also included. Both of the new complexes display two distinct band types. The first of these bands, between 300 and 330 nm, has very large absorption coefficient and, by analogy to **1**$^{2+}$ and other bpta complexes,[19,20] is assigned to ligand-centered $\pi-\pi^*$ transitions.

Less-intense bands observed between 500 and 750 nm are assigned to ^{3}MLCT transitions involving the pyridyl and tetrazine moieties of the bridging ligand. It is noticeable that the energy of these latter bands seems to be dependent on the thiacrown coordinated to the metal center: for complex **2**, which contains [Ru([12]aneS$_4$)] metal centers, two bands centered at 528 and 716 nm are observed, while analogous transitions for **1**[12] and **3**, are merged due to a bathochromic shift of the higher-energy band.

Electrochemical Studies. The electrochemical properties of **1** have been reported before.[12] Cyclic voltammetry (CV) studies were carried out on the new complexes in acetonitrile solvent with 0.1 M Bu_4NPF_6 as the support electrolyte.

Within the MeCN solvent window, complexes **2** and **3** display three redox couples that show good reversibility. For previously reported dinuclear complexes,[12,19,20] such as **1**, two separate redox processes that are anodic relative to Ag/AgCl are observed and these are assigned to Ru$^{II/III}$ couples—for **1**, $\Delta E_{1/2}$ for the oxidations is 480 mV—while a reversible couple observed at very low cathodic voltages vs Ag/AgCl (−0.049 V for **1**) is assigned to a low-lying reduction of the tetrazine ring of bpta. For complexes **2** and **3**, redox couples are observed at very different potentials, Table 6; to aid comparison, the previously reported data for **1** are also included.

The new complexes display a couple at ca. −0.95 V. By comparison with previously reported systems, this is assigned to reduction of the pyridyl moieties of the bridging ligand.

(18) Champness, N. R.; Kelley, P. F.; Levason, W.; Reid, G.; Slawin, A. M. Z.; Williams, D. J. *Inorg. Chem.* **1995**, *34*, 651.
(19) Johnson, J. E. B.; de Groff, C.; Ruminski, R. R. *Inorg. Chem. Acta* **1991**, *187*, 73. Poppe, J.; Moscherosch, M.; Kaim, W. *Inorg. Chem.* **1993**, *327*, 2640.
(20) Ernst, S.; Ksack, V.; Kaim, W. *Inorg. Chem.* **1988**, *27*, 1146. Kaim, W.; Ernst, S.; Ksack, V. *J. Am. Chem. Soc.* **1990**, *112*, 17.

Table 6. Summary of Electrochemical Data

complex[a]	$E_{1/2}$(**1**) (V)	$E_{1/2}$(**2**) (V)	$E_{1/2}$(**3**) (V)
1[b]	−0.049	1.36	1.84
2	−0.93	0.26	1.80
3	−0.95	0.37	1.85

[a] Carried out under a dinitrogen atmosphere. Support electrolyte: 0.1 M $[NBu_4][PF_6]$ in MeCN, $\nu = 200$ mV s^{-1}. vs Ag/AgCl reference electrode. All couples are reversible with $\Delta E \leq 100$ mV and $|I_{Pa}/I_{Pc}| = 1$. [b] Data from ref 12.

However, in contrast to previous reports, bpta/bpta$^{\bullet-}$ (tetrazine-based) reductions at cathodic voltages close to zero are not observed. Furthermore, while two anodic couples are observed, the first is at an unusually low potential of <0.40 V, while the second is at 1.8−1.9 V. More anodic sweeps, up to the limit of the MeCN redox window (ca. 2.2 V vs Ag/Ag^+), reveal no further redox processes.

It is established that thiacrown ligands are π-acceptor ligands that stabilize low oxidation states; given this fact and the low potential of the first anodic process for complexes **2** and **3**, it seems unlikely that this is a metal-based couple. If it were, this would imply that for each of the complexes, $\Delta E_{1/2}(1,2)$ would take an unprecedentedly large value above 1.5 V. Thus, this process is assigned to a bpta/bpta$^{\bullet-}$-based couple, which has been shifted by >0.3 V compared to previously reported systems such as **1**. This suggests that, at least in the dry, anaerobic conditions employed in CV experiments and at 0 V vs Ag/AgCl, the metal complexes formally contain a reduced radical anion bridging ligand. Therefore, the second anodic process observed for **2** and **3** can be assigned to the first metal-based oxidation couple. Certainly this latter assignment is consistent with previous studies on monometallic $[Ru^{II}([n]aneS_4)]$ systems which have revealed large anodic shifts in metal-based oxidations; for example the $Ru^{III/II}$ oxidation couple for $[Ru^{II}([12]aneS_4)(bpy)]^{2+}$ (where bpy = 2,2′-bipyridine) is observed above 1.5 V vs Ag/AgCl.[16b]

A second metal-based oxidation couple is not observed in these experiments. This is unsurprising: as can be seen from the data summarized in Table 6, $\Delta E_{1/2}(1,2)$ for **1** is 480 mV. Analogous electrochemical coupling for **2** and **3** implies the occurrence of a second $Ru^{III/II}$ couple at >2.3 V, a potential beyond the MeCN redox window. To gain further insights into the redox properties of the new systems, complexes **2** and **3** were investigated using UV/vis/NIR spectroelectochemistry.

Spectroelectrochemistry Studies. Spectroelectrochemistry was carried out on hexafluorophosphate salts under a dinitrogen atmosphere in acetonitrile using an optically transparent thin-layer electrochemical, OTTLE cell thermostated at 253 K. All redox couples were fully reversible, as shown by the presence of clean isosbestic points during interconversions.

It was found that the application of a voltage of 0 V to a solution of **2** led to a redox process. During this process, bands at 716 and 528 nm assigned to MLCT almost completely collapse and a new band at 495 nm appears, while a $\pi-\pi^*$ band at 308 nm shows a hypsochromic shift to 289 nm, Figure 4.

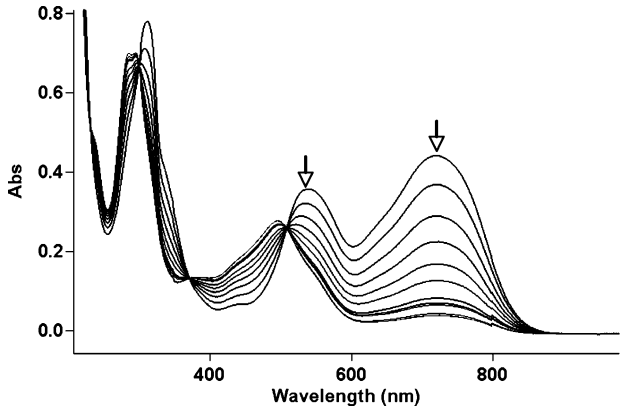

Figure 4. OTTLE plot of redox processes occurring for complex **2** at 0.00 V vs Ag/AgCl.

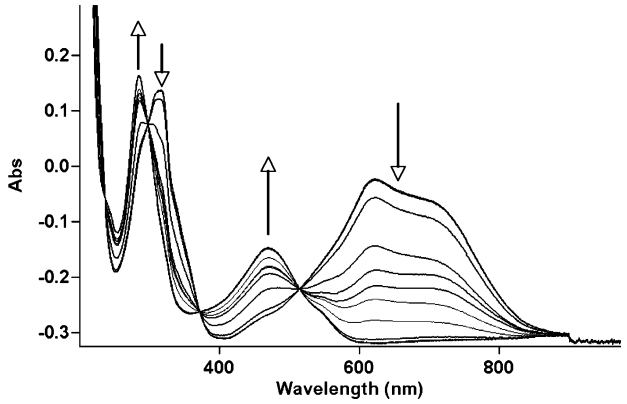

Figure 5. OTTLE plot showing reduction of $\mathbf{3}^{4+}$ at +0.00 V vs Ag/AgCl.

However, on application of a potential more than the first anodic couple observed in the CV of **2**, an exact mirror image of the process observed in Figure 4, occurs with the growth of bands at 528 and 716 nm and a collapse of the band at 495 nm.

Previously reported spectroelectrochemistry studies on **1** have confirmed that reduction of $\mathbf{1}^{2+}$ results in the formation of a tetrazine-based radical anion and that the band at 751 nm assigned to Ru → bpta ^{3}MLCT collapses during this reduction process.[12] The spectral changes observed for **2** at 0 V closely resemble those observed during the reduction of $\mathbf{1}^{2+}$. These observations confirm that, in normal atmospheric conditions that are relatively oxidizing, the complex exists as $\mathbf{2}^{4+}$, but under an inert atmosphere and at 0 V vs Ag/AgCl, the complex is reduced to $\mathbf{2}^{3+}$, forming a system consisting of two Ru^{II} centers, bridged by the monoreduced, radical anion bpta$^{\bullet-}$.

Studies on **3** reveal that a similar $\mathbf{3}^{4+/3+}$ reduction couple is also observed for this complex when it is held at a potential of 0 V vs Ag/AgCl in an inert atmosphere. Again, the formation of $\mathbf{3}^{3+}$ is accompanied by a collapse of low-energy MLCT bands and the growth of a higher-energy band, in this case centered at 472 nm, Figure 5. Similar hypsochromic shifting of MLCT bands during metal complex reductions has been commonly observed. As for $\mathbf{2}^{3+}$, the first oxidation of $\mathbf{3}^{3+}$ results in an exact reversal of all the changes observed in Figure 6, confirming that this anodic process is also due to the [bpta/bpta$^{\bullet-}$] couple.

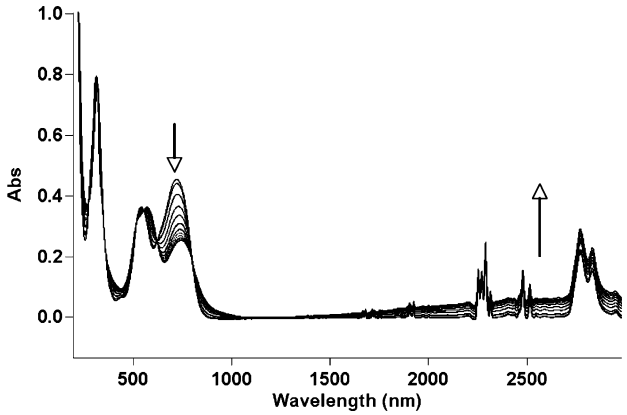

Figure 6. OTTLE plot showing the oxidation of $\mathbf{2}^{4+}$ to $\mathbf{2}^{5+}$ at +2.0 V in acetonitrile.

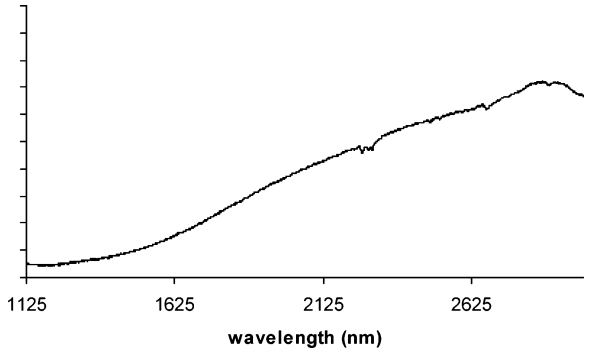

Figure 7. Detail of difference spectra of [$\mathbf{2}^{5+} - \mathbf{2}^{4+}$].

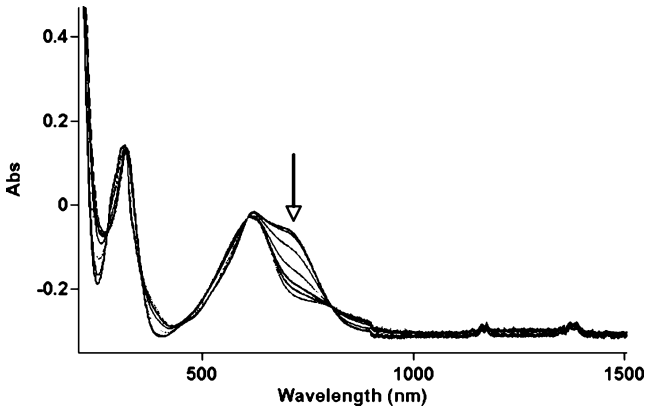

Figure 8. OTTLE plot showing the oxidation of $\mathbf{3}^{4+}$ to $\mathbf{3}^{5+}$ at 2.0 V in acetonitrile.

The most noticeable feature observed during oxidation of $\mathbf{2}^{4+}$ to $\mathbf{2}^{5+}$ is, again, a reduction in the intensity of the MLCT band at 716 nm. However, although obscured by solvent transitions, there is also clear evidence of the growth of a broad, lower-intensity band centered at much lower energies, Figure 6. This NIR band is more clearly resolved in the [$\mathbf{2}^{3+} - \mathbf{2}^{4+}$] difference spectrum, Figure 7.

Although the lower-energy side of the band extends outside the range of the spectrometer, the band appears to be Gaussian with a maximum ($\epsilon \approx 3700$ dm^3 mol^{-1} cm^{-1}) centered at very low energy, ca. 2850 nm ($\sim$3500 cm^{-1}). The energy, intensity, and form of this band are consistent with intervalence charge-transfer, IVCT.

Assuming Gaussian band shape and using the high-energy side of the transition, Hush theory[21] reveals that the calculation $\nu_{1/2} = (2310\nu)^{1/2}$ cm^{-1}, yields $\nu_{1/2}$ ($\mathbf{2}^{5+}$, calcd) = 2847 cm^{-1}, where $\nu_{1/2}$ is the width at half-height of the IVCT band maximum. Within experimental error, this value very closely matches the experimentally derived $\nu_{1/2}$ of ca. 2780 cm^{-1}. Therefore, it seems likely that this complex is a Robin and Day Class II (valence trapped/electron hopping) system, perhaps verging on class II/III behavior, and consequently, an estimate of H_{AB} can be obtained by[1]

$$H_{AB} = \frac{2.05 \times 10^{-2}}{R}(\nu_{max}\,\epsilon_{max}\,\nu_{1/2})^{1/2}$$

Where R, the transition dipole length (the distance through which the charge is carried), is approximated by the intermetallic distance of 6.806 Å, obtained from the X-ray structure of $\mathbf{2}^{4+}$. Using the experimental data, H_{AB} is calculated to be 575 cm^{-1}. This value contrasts with the results obtained for $\mathbf{1}^{5+}$, which was found to be a Class III delocalized system,[12] with $H_{AB} = 2688$ cm^{-1}

The corresponding oxidation of $\mathbf{3}^{4+}$ results in a drop in intensity of the low-energy shoulder of the MLCT band, Figure 8. However, the low-energy region of the spectrum was very noisy and no IVCT could be discerned. It may be that the IVCT is still further shifted outside the window of the spectrometer used. Conversely, previous reports have demonstrated that even Class III valence-delocalized systems incorporating bpta as a bridge can display very weak IVCT bands.[19,20,22] Given this latter observation, it is possible the IVCT of $\mathbf{3}^{5+}$ is too broad and/or weak to be detectable.

Conclusions

It is clear that substitution of the [RuCl([9]aneS$_3$] center used in **1** with [Ru([*n*]aneS$_4$] moieties has had profound effects on the physical properties of the studied systems. Electronically, the change in metal centers has clearly resulted in a reduction in intermetallic coupling. Electrochemically, the most distinctive changes are the anodic shift of the bpta/bpta$^{\bullet-}$ couple and an even larger anodic shift in the Ru$^{III/II}$ couple. This change in the potential of the bpta/bpta$^{\bullet-}$ couple has meant that the ligand, which has previously behaved as an innocent bridging ligand for the construction of Ru$^{III/II}$ MV systems has now begun to behave in a distinctively noninnocent manner. All these changes can all be explained by a consideration of the bonding properties of thiacrown ligands.

From simple electrostatic arguments, the oxidation of Ru^{II} centers in the tetracations $\mathbf{2}^{4+}$ and $\mathbf{3}^{4+}$ would be expected to be anodically shifted compared to that of the dication $\mathbf{1}^{2+}$. However, the first Ru^{II} oxidations of $\mathbf{2}^{4+}$ and $\mathbf{3}^{4+}$ are also considerably anodically shifted compared to analogous tetracations; for example, [{Ru(bpy)$_2$}$_2$bpta]$^{4+}$ displays a first Ru^{II}-based couple at 1.52 V.[19] Clearly, another factor must also contribute to the large changes in the electrochemical behavior of $\mathbf{2}^{4+}$ and $\mathbf{3}^{4+}$ compared to $\mathbf{1}^{2+}$.

(21) Hush, N. S. *Prog. Inorg. Chem.* **1967**, *8*, 391. Hush, N. S. *Electrochim. Acta* **1968**, *13*, 1005. Hush, N. S. *Coord. Chem. Rev.* **1985**, *64*, 135.
(22) Gordon, K. C.; Burrell, A K.; Simpson, T. J.; Page, S. E.; Kelso, G.; Polson M. I. J.; Flood, A. *Eur. J. Inorg. Chem.* **2002**, 554.

It has been known that thiacrowns are poor σ-donors but good π-acid ligands.[23] The substitution of the π-donor chloride ligand in **1** with π-accepting thiacrown-based sulfur ligands in complexes **2** and **3** results in a decrease of electron density on the metal center, thus stabilizing the Ru^{II} oxidation state. However, this effect means the Ru^{II} metal center accepts more electron density from the already electron-deficient tetrazine ring of the bpta bridge, thus destabilizing the oxidized form of this ligand with respect to the radical anion form. Increased back-bonding to the thiacrowns would also lower electron density available for delocalization over the bridging ligand and, as has been seen before,[10] this leads to a lowering of intermetallic electronic coupling.

Further studies on the electronic properties of these complexes are currently underway, while related systems with multiple metal and ligand redox states are also being constructed.

Experimental Section

Materials. All chemicals were obtained from commercial sources and were used as supplied unless otherwise stated. 3,6-bis(2-pyridyl)-1,2,4,5-tetrazine and [{RuCl(DMSO)([*n*]aneS$_4$)}][PF$_6$] were synthesized using published methods.[14,15] Solvents were obtained from commercial sources and were dried and purified using standard literature methods. All reactions were carried out under a nitrogen atmosphere unless otherwise stated.

Physical Measurements. Microanalyses for carbon, hydrogen, nitrogen, and sulfur were obtained using a Perkin-Elmer 2400 analyzer, working at 975 °C. ^{1}H NMR spectra were recorded on a Bruker AM250 machine, working in Fourier transform mode. Mass spectra were obtained on a Kratos MS80 in positive-ion mode with a *m*-nitrobenzyl alcohol matrix. UV/vis spectra were recorded on a Unicam UV2 spectrometer in twin beam mode. Spectra were recorded in matched quartz cells and baseline corrected. CV was carried out using an EG&G Versastat II potentiostat and the Condecon 310 hardware/software package. Measurements were made using $\sim 2 \times 10^{-3}$ mol dm^{-3} solutions in dry solvents under a nitrogen atmosphere with support electrolyte as stated. Potentials were measured with reference to a Ag/AgCl electrode. Ferrocene was used as an internal reference. UV/vis/NIR spectroelectrochemical measurements were performed in acetonitrile using an OTTLE cell mounted in a Cary-5000 UV/vis/NIR spectrometer and thermostated at 253 K.

Syntheses. Improved Preparation of [{RuCl([9]aneS$_3$)}$_2$-μ-bpta][(PF$_6$)$_2$], [1](PF$_6$)$_2$. To a solution of 0.3 g (0.697 mmol) of [Ru([9]aneS$_3$)(DMSO)Cl$_2$] in 20 mL of ethanol/water, 1:1, was added 3,6-bis(2-pyridyl)-1,2,4,5-tetrazine (0.0823 g, 0.5 equiv), and the reaction mixture was brought to reflux for 3 h. Excess NH_4PF_6 (0.114 g, 3 equiv) was added to the warm solution, resulting in a precipitate that was quickly filtered, washed with water and ethanol, and then dried in vacuo. No further purification was needed. Yield = 0.22 g (55%).

Preparation of [{Ru([12]aneS$_4$)}$_2$-μ-bpta][(PF$_6$)$_4$], [2](PF$_6$)$_4$. [RuCl(DMSO)([12]aneS$_4$)]PF$_6$ (0.3 g, 0.5 mmol) was refluxed in 20 mL of ethanol/water, 1:1, in the presence of $AgNO_3$ (0.11 g, 1.3 equiv) for 4 h. After removal of AgCl by filtration, bpta (0.059 g, 0.5 equiv) was added and the reaction mixture was refluxed for a further 3 h. Excess NH_4PF_6 (0.4075 g, 5 equiv) was added to the warm solution, resulting in a precipitate, which was quickly filtered and then washed with water and ethanol and then dried in vacuo. No further purification was needed. Yield = 0.214 g (57%). ^{1}H NMR (CD_3NO_2): δ_H = 3.06−4.47 (m, 32H), 8.05 (dd, 2H), 8.43 (dd, 2H), 8.95 (d, 2H), 9.65 (d, 2H). MS; *m*/*z* (%):1355 (100) [M − PF$_6$]. Anal. Calcd for $Ru_2C_{28}H_{40}N_6S_8P_4F_{24}$ (1500): C = 22.43%, H = 2.69%, S = 17.11%, N = 5.61%; found: C = 22.75%, H = 2.21%, S = 16.86%, N = 5.34%

Preparation of [{Ru([14]aneS$_4$)}$_2$-μ-bpta][(PF$_6$)$_4$], [3](PF$_6$)$_4$. [RuCl(DMSO)([14]aneS$_4$)]PF$_6$ (0.3 g, 0.478 mmol) was refluxed in 20 mL of ethanol/water, 1:1, in the presence of $AgNO_3$ (0.106 g, 1.3 equiv) for 4 h. After removal of AgCl by filtration, bpta (0.056 g, 0.5 equiv) was added and the reaction mixture was refluxed for a further 3 h. Excess NH_4PF_6 (0.39 g, 5 equiv) was added to the warm solution, resulting in a precipitate, which was quickly filtered and then washed with water and ethanol and then dried in vacuo. No further purification was needed. Yield = 0.208 g (56%). ^{1}H NMR (CD_3NO_2): δ_H = 2.46−4.08 (m, 40H), 8.12 (dd, 2H), 8.47 (dd, 2H), 8.96 (d, 2H), 9.52 (d, 2H). MS; *m*/*z* (%): 1411 (34) [M+ −PF$_6$]. Anal. Calcd $Ru_2C_{32}H_{48}N_6S_8P_4F_{24}$ (1556): C = 24.71%, H = 3.11%, S = 16.49%, N = 5.40%; found: C = 25.29%, H = 3.01%, S = 16.94%, N = 5.21%.

Crystals of [**1**](PF$_6$)$_2$, [**2**](PF$_6$)$_4$, and [**3**](PF$_6$)$_4$ were grown by vapor diffusion using nitromethane and diethyl ether mixtures. Crystallographic data are summarized in Table 1. In all three cases, data were collected at 150 K on a Bruker Smart CCD area detector with an Oxford Cryosystems low-temperature system and refined with the program package SHELXTL[24] as implemented on the Viglen Pentium computer. Hydrogen atoms were placed geometrically and refined with a riding model and with U_{iso} constrained to be 1.2 times U_{eq} of the carrier atom.

Acknowledgment. M.N. is grateful for the award of an EPSRC Quota studentship. J.A.T. and M.D.W. are also are grateful for financial support from EPSRC. J.A.T. acknowledges the support of The Royal Society.

Supporting Information Available: Crystallographic information files for the structures of [**2**](PF$_6$)$_2$, [**2**](PF$_6$)$_4$, and [**3**](PF$_6$)$_4$. This material is available free of charge via the Internet at http://pubs.acs.org.

IC051151B

(23) Mullen, G. E. D.; Went, M. J.; Wocaldo, S.; Powell, A. K.; Blower, P. J. *Angew. Chem., Int. Ed. Engl.* **1997**, *36*, 1205. Mullen, G. E. D.; Fassler, T. F.; Went, M. J.; Howland, K.; Stein, B.; Blower, P. J. *J. Chem. Soc., Dalton Trans.* **1999**, 3759.

(24) SHELXTL, An integrated system for solving and refining crystal structures from diffraction data (Revision 5.1), Bruker AXS LTD.